nm results directly from dissociation of ketene, and 15% of the $^3B_1$ is formed by collisional deactivation of $^1A_1$.[36]

Acknowledgment. This research was supported by the U.S. Energy Research and Development Association under Contract No. AT 11-1 2026.

Supplementary Material Available: Discussion of intensity effects, and three figures (5 pages). Ordering information is given on any current masthead page.

References and Notes

(1) J. W. Simons and B. S. Rabinovitch, *J. Phys. Chem.*, **68**, 1322 (1964).
(2) S. Ho, I. Unger, and W. A. Noyes, Jr., *J. Am. Chem. Soc.*, **87**, 2297 (1965); S. Ho and W. A. Noyes, Jr., *ibid.*, **89**, 5901 (1967).
(3) R. W. Carr, Jr., and G. B. Kistiakowsky, *J. Phys. Chem.*, **70**, 118 (1966); T. W. Eder and R. W. Carr, Jr., *ibid.*, **73**, 2074 (1969).
(4) H. M. Frey, *Chem. Commun.*, 260 (1965).
(5) F. S. Rowland, *Discuss. Faraday Soc.*, 124 (1972).
(6) G. B. Kistiakowsky and T. A. Walter, *J. Phys. Chem.*, **72**, 3952 (1968).
(7) G. B. Kistiakowsky and B. B. Saunders, *J. Phys. Chem.*, 77, 427 (1973).
(8) R. Hoffmann, *J. Am. Chem. Soc.*, **90**, 1475 (1968).
(9) W. Kirmse, "Carbene Chemistry", 2nd ed, Academic Press, New York, N.Y., 1971, Chapter 8.
(10) J. F. Harrison, *Acc. Chem. Res.*, 7, 378 (1974).
(11) E. B. Klunder and R. W. Carr, Jr., *J. Am. Chem. Soc.*, **95**, 7386 (1973).
(12) See paragraph at end of text regarding supplementary material.
(13) Computed from $\Delta H_f°_{298}(CH_2CO) = -11.4$ kcal/mol [R. L. Nuttall, A. H. Laufer, and M. V. Kilday, *J. Chem. Thermodyn.*, **3**, 167 (1971)]; $\Delta H_f°_{298}(CH_2\ ^3B_1) = 95 \pm 1$ kcal/mol [H. Prophet, *J. Chem. Phys.*, **38**, 2345 (1963)]; $\Delta H_f°_{298}(CO) = -26.4$ kcal/mol [F. D. Rossini, "Selected Values of Physical and Thermodynamic Properties of Hydrocarbons and Related Compounds", API Project 44, Carnegie Press, New York, N.Y., 1953].
(14) R. N. Dixon and G. H. Kirby, *Trans. Faraday Soc.*, **62**, 1406 (1966); A. H. Laufer and R. A. Keller, *J. Am. Chem. Soc.*, **93**, 61 (1971).
(15) M. L. Halberstadt and J. R. McNesby, *J. Am. Chem. Soc.*, **89**, 4317 (1967).
(17) W. L. Hase, R. J. Phillips, and J. W. Simons, *Chem. Phys. Lett.*, **12**, 161 (1971).
(18) H. M. Frey, *J. Chem. Soc., Chem. Commun.*, **18**, 1024 (1972).
(19) D. R. McLaughlin, C. F. Bender, and H. F. Schaefer III, *Theor. Chim. Acta*, **25**, 352 (1972).
(20) P. J. Hay, W. J. Hunt, and W. A. Goddard III, *Chem. Phys. Lett.*, **13**, 30 (1972).
(21) V. Staemmler, *Theor. Chim. Acta*, **31**, 49 (1973).
(22) G. Herzberg and J. W. C. Johns, *Proc. R. Soc. London, Ser. A*, **295**, 707 (1966).
(23) See the listing of eight computations of $E(^1B_1) - E(^1A_1)$ given in ref 10.
(24) G. Herzberg, "Electronic Spectra of Polyatomic Molecules", Van Nostrand, Princeton, N.J., 1967, p 583.
(25) S. Y. Chu, A. K. Q. Siu, and E. F. Hayes, *J. Am. Chem. Soc.*, **94**, 2969 (1972).
(26) R. L. Russell and S. F. Rowland, *J. Am. Chem. Soc.*, **90**, 1671 (1968).
(27) R. Kushner and F. S. Rowland, *J. Am. Chem. Soc.*, **91**, 1539 (1969).
(28) C. McKnight, P. S. T. Lee, and F. S. Rowland, *J. Am. Chem. Soc.*, **89**, 6802 (1967).
(29) J. D. Rynbrandt and B. S. Rabinovitch, *J. Phys. Chem.*, **74**, 1679 (1970).
(30) T. W. Eder and R. W. Carr, Jr., *J. Chem. Phys.*, **53**, 2258 (1970).
(31) The difference in intensity between 313 and 213.9 nm is insufficient for this to be an artifact of intensity, obscuring large yields of radicals.
(32) W. Braun, A. M. Bass, and M. Pilling, *J. Chem. Phys.*, **52**, 5131 (1970).
(33) P. S. T. Lee, R. L. Russell, and F. S. Rowland, *J. Chem. Soc. D.*, 18 (1970).
(34) H. M. Frey and R. Walsh, *J. Chem. Soc. D*, 2115 (1970).
(35) R. W. Carr, Jr., *J. Phys. Chem.*, **76**, 1581 (1972).
(36) V. P. Zabransky and R. W. Carr, Jr., *J. Phys. Chem.*, in press.

The Inversion Barrier in AH_3 Molecules

William Cherry* and Nicolaos Epiotis

Contribution from the Department of Chemistry, University of Washington, Seattle, Washington 98195. *Received February 18, 1975*

Abstract: A one-electron approach is used to rationalize the trends in the inversion barriers of AH_3 molecules as the central atom is varied. The large increase in the barrier as A is changed from a second- to a third-row element and the substituent electronegativity effect upon the height of the barrier can be traced to a single MO interaction which obtains in AH_3 molecules.

In the AH_3 isoelectronic series with eight valence electrons, the barrier to inversion increases dramatically as the central atom is changed from a second-row to a third-row element.[1] For example, the inversion barrier of NH_3 is 5.78 kcal/mol,[2] while the inversion barrier of PH_3 is 37.2 kcal/mol,[3] the difference indicating an effect of extremely large magnitude. The experimentally determined barriers to inversion for several other molecules are shown in Table I. While the preferred pyramidal geometry of AH_3 molecules is adequately rationalized by simple MO theory, one can confidently state that no theoretical explanation of the relationship between the electronic nature of the central atom and the magnitude of the barrier has been advanced. In this paper, we present a one-electron MO approach that is capable of rationalizing the observed trend of the magnitude of the inversion barrier in the AH_3 isoelectronic series.

First, we shall briefly review the factors which seem to be responsible for the nonplanar geometry of AH_3 molecules.[4] The correlation diagram for the planar and pyramidal forms of a typical AH_3 molecule is shown in Figure 1. Since the system has eight valence electrons, the highest occupied MO (HOMO) in either the planar or pyramidal form is a "lone pair" MO. Upon bending, the lowest valence MO(A_1) is changed little in energy and its effect on geometry preference is negligible. On the other hand, the energy of the degenerate pair of MO's (E) increases, and this increase has been ascribed to two effects: first, there is a decrease in the in-phase (bonding) overlap between the central atoms p AO's and the 1s atomic orbitals of the hydrogen, and, secondly, there is an increase in the out-of-phase (antibonding) overlap of any two hydrogens as they are moved closer together. Finally, the energy of the HOMO of the planar AH_3 molecule decreases considerably upon pyramidalization due to its mixing with the lowest unoccupied MO (LUMO) which is a σ^*-type MO. Since the energy lowering of the lone pair MO is greater than twice the energy increase of one of the degenerate MO's, the molecule assumes a nonplanar geometry. *The extent of interaction between the HOMO and LUMO in these molecules determines not only the geometry but also, as we shall see, the inversion barrier.*

Perturbation theory[5] provides a convenient framework for discussing orbital interactions. If there is no degeneracy

* Standard Oil Predoctoral Fellow

Table I. Experimentally Determined Inversion Barriers for Several Molecules

(a)	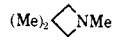	8.8[a]
(b)	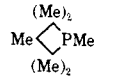	~40[b]
(c)	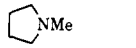	8.4[c]
(d)	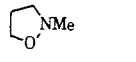	16.9[d]
(e)	$(C_6H_5CH_2)_2N-Me$	6.5[e]
(f)	$(C_6H_5CH_2)_2N-OH$	12.8[f]
(g)	$(C_6H_5)(p\text{-}CH_3C_6H_4)P-Me$	30.3[g]

[a] J. M. Lehn and J. Wagner, *Chem. Commun.*, 148 (1968). [b] S. E. Cramer, R. J. Chorvht, C. H. Chan, and D. W. Davis, *Tetrahedron Lett.*, 5799 (1968). [c] J. B. Lambert, W. L. Oliver, and B. S. Packard, *J. Am. Chem. Soc.*, 93, 933 (1971). [d] F. G. Riddell, J. M. Lehn, and J. Wagner, *Chem. Commun.*, 1403 (1968). [e] L. H. Bushweller and J. W. O'Neil, *J. Am. Chem. Soc.*, 92, 2159 (1970). [f] J. R. Fletcher and I. O. Sutherland, *Chem. Commun.*, 687 (1970). [g] K. Mislow and R. D. Baechler, *J. Am. Chem. Soc.*, 92, 3060 (1970).

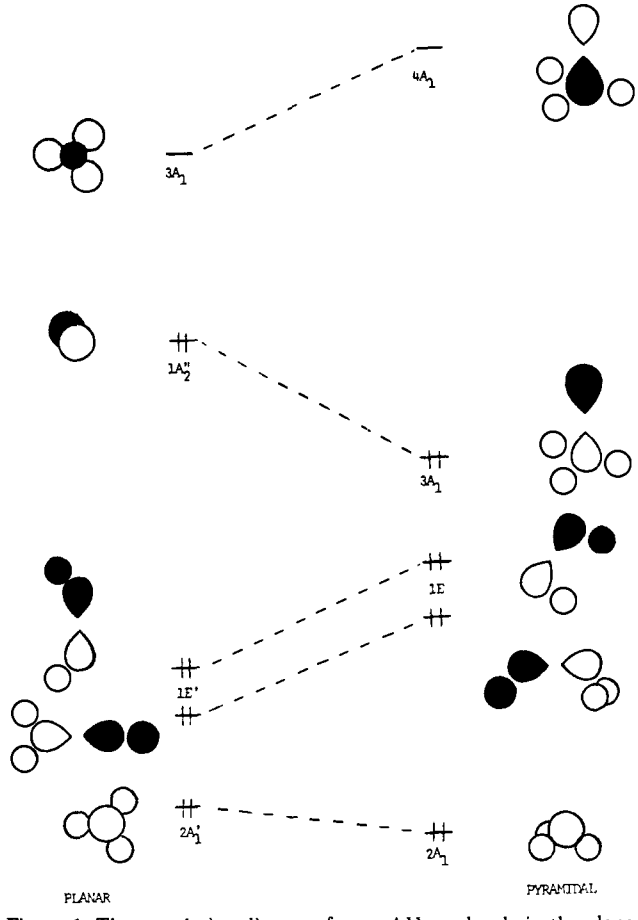

Figure 1. The correlation diagram for an AH_3 molecule in the planar and pyramidal geometries. Ammonia was taken as a typical example.

between the interacting MO's, which will be the case of interest to us, the change in energy of orbital ϕ_m due to its interaction with orbital ϕ_n is given by the expression

$$\Delta E_m = \langle \phi_m | H | \phi_n \rangle^2 / (E_m - E_n) \quad (1)$$

where E_m and E_n are the unperturbed energies of ϕ_m and ϕ_n, respectively. The off-diagonal matrix element may be approximated by the Longuet-Higgins and Roberts[6] equation

$$\langle \phi_m | H | \phi_n \rangle = k \langle \phi_m | \phi_n \rangle = k S_{mn} \quad (2)$$

where S_{mn} is the overlap integral. Substituting into eq 1 gives

$$\Delta E_m = (k S_{mn})^2 / (E_m - E_n) \quad (3)$$

We shall now apply these theoretical arguments to the case of AH_3 molecules and inquire how the magnitude of their inversion barrier depends on the nature of A.[7] Our approach is best illustrated by comparing NH_3 and PH_3. In the planar geometry, the HOMO and the LUMO cannot interact because they are mutually orthogonal. However, as pyramidalization occurs, the two orbitals begin to interact, and the magnitude of their interaction is inversely proportional to their energy separation and directly proportional to the square of their overlap (see eq 3). We have carried out CNDO/2[8] calculations of the planar NH_3 and PH_3 molecules to determine the initial HOMO/LUMO energy separation as well as the HOMO/LUMO eigenvectors and also CNDO/2 calculations of the pyramidal NH_3 and PH_3 molecules in order to determine the appropriate AO overlap integrals. The calculations of these overlap integrals were carried out in two different ways: (a) calculations assuming the NH_3 and PH_3 molecules to be in their experimentally determined geometries (experimental geometry model);[9] (b) calculations assuming the NH_3 and PH_3 to have a common pyramidal geometry (standard geometry model). Both models were found to lead to identical qualitative trends.

The CNDO/2 calculations revealed that the HOMO and LUMO in planar PH_3 are much closer energetically than in NH_3. The eigenvalues for both planar molecules are shown in Figure 2. The actual differences are 0.4143 and 0.8245 au for PH_3 and NH_3, respectively. Clearly, the energy-separation factor favors a greater HOMO/LUMO interaction in PH_3 than in NH_3. The overlap factor also favors a greater HOMO/LUMO interaction in PH_3. The overlap integral between the central atom p_z AO and σ^* is given by

$$\begin{aligned} \langle Ap_z | \sigma^* \rangle &= \langle Ap_z | c_A As - c_1 H_1 s - c_2 H_2 s - c_3 H_3 s \rangle \\ &= 3c_1 \langle Ap_z | H_1 s \rangle \end{aligned} \quad (4)$$

where c_i is the atomic orbital coefficient of the ith hydrogen 1s AO, and c_A is the atomic orbital coefficient of ns AO of A in the σ^* MO. Due to symmetry, all the hydrogens will have the same coefficients, i.e., $c_1 = c_2 = c_3$. These coefficients were obtained from the calculations of the planar form. Using the experimental geometry model, the actual calculated values for the $\langle Ap_z | \sigma^* \rangle$ overlap integrals are 0.4182 and 0.2000 for PH_3 and NH_3, respectively. Using the above values for the energy difference and overlap integral of the interacting orbitals, we can calculate the stabilization energy which accompanies pyramidalization by means of eq 3. The stabilization energy in the case of NH_3 is found to be 0.1034, while that of PH_3 is 0.8988. That is, the stabilization of the lone pair as a result of pyramidalization is much greater for PH_3 than for NH_3. This is the primary cause of the increased barrier as the central atom is changed from N to P.

As mentioned above, the trend in the stabilization of the lone pair is independent of the model used in calculating the overlap integral between the HOMO and LUMO. If the stabilization energies of NH_3 and PH_3 are calculated using the standard geometry model with an HAH angle of 109.5°, the computed values become 0.1034 and 0.3034 for NH_3 and PH_3, respectively. In addition, it should be mentioned that, in all cases, the energy of the LUMO was taken from the calculation of the planar molecule. As bending occurs, this MO would decrease in energy if it had not mixed with the HOMO. The energy decrease is due to the increased overlap of the in-phase hydrogen AO's. For NH_3

Table II. Theoretical and Experimental Ionization Potentials for NH_3 and PH_3

	Ionization potentials, au		
	Ab initio	CNDO/2[a]	Experimental
NH_3			
Planar	0.3908[b,c]	0.5456[d]	
Pyramidal	0.4278[b,c]	0.5898[d]	0.3735[e]
PH_3			
Planar	0.3005[f,c]	0.3964[d]	
Pyramidal		0.4556[d]	
Pyramidal	0.3867[f,g]	0.5081[g]	0.3640[e]

[a] This work. [b] Reference 11. [c] Optimized geometry used in the calculations. [d] Standard geometry used in the calculations. [e] D. W. Turner, C. Baker, A. D. Baker, and C. R. Brundle, "Molecular Photoelectron Spectroscopy", Wiley-Interscience, Inc. New York, N.Y., 1970. [f] Reference 10. [g] Experimental geometry used in the calculations.

Table III. Stabilization Energies for AH_3 Pyramidalization and Theoretical and Experimental Inversion Barriers

	Stabilization energy of HOMO	Inversion barrier[b]		
		Ab initio	CNDO/2	Experimental
CH_3^-	0.1238	5.46	17.8	
SiH_3^-	0.2982	39.6		
NH_3	0.1034	5.08	13.5	5.78
	(0.1034)[a]	5.08	13.5	5.78
PH_3	0.3034			
	(0.8988)[a]	37.2		
OH_3^+	0.0770		0.1	
SH_3^+	0.2456	30.0	29.3	

[a] The stabilization energy in parentheses was calculated using the experimental geometry. [b] Cited in ref 1.

and PH_3, the increase of the overlap integral between any two of the hydrogens is 0.0306 and 0.0162, respectively, if standard geometries are used, and 0.0306 and 0.0652 if experimental geometries are used. This leaves some uncertainty as to the exact unperturbed energy that should be used for the LUMO in these calculations. In the second case where experimental geometries are used, the LUMO of the PH_3 decreases in energy more than the LUMO of NH_3 and will consequently only reinforce our conclusions. In the first case, the LUMO of NH_3 will decrease slightly more in energy. However, in both cases this change in energy is small and is not expected to have a large effect upon the difference between the HOMO/LUMO energy separation in NH_3 and PH_3.

An index of the relative magnitude (and, hence, the accompanying stabilization) of the HOMO-LUMO interaction upon pyramidalization in NH_3 and PH_3 is provided by the ionization potentials of these two molecules in their equilibrium geometry. In their planar form, the phosphorus lone pair is less tightly bound than the nitrogen lone pair and, thus, according to Koopman's theorem, the energy of the NH_3 HOMO is much lower than the energy of the PH_3 HOMO, their difference being 0.1492 au according to CNDO/2 and 0.0903 au according to ab initio calculations. The calculated ionization potentials are shown in Table II. As pyramidalization occurs, the HOMO-LUMO interaction in PH_3 is much greater than that in NH_3 and tends to depress the energy of the PH_3 HOMO much more than the energy of the NH_3 HOMO; e.g., as pyramidalization occurs, the relative energy of the NH_3 and PH_3 HOMO's tend to be reversed. The energy difference between these two orbitals is 0.1342 (or 0.0817) au according to CNDO/2 and 0.0411 au according to ab initio[10,11] and only 0.26 eV (0.0096 au) according to experiment.

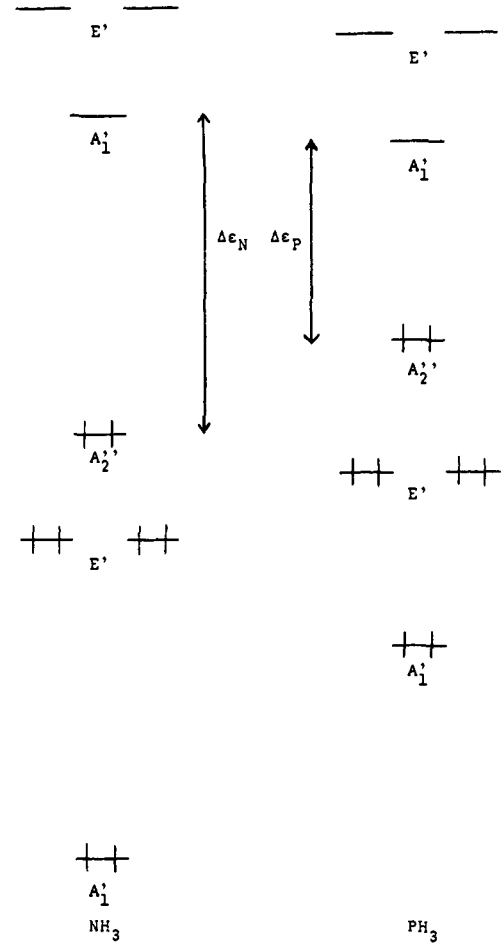

Figure 2. The relative energies of the valence MO's for planar NH_3 and PH_3 as calculated by CNDO/2 methods. The energy difference between the HOMO and LUMO ($\Delta\epsilon$) is indicated ($\Delta\epsilon_N > \Delta\epsilon_P$).

These simple ideas can be extended to include all the members in this isoelectronic series, i.e., CH_3^-, SiH_3^-, NH_3, PH_3, OH_3^+, and SH_3^+. We have performed the same type of calculations on all members in this series. The results are shown in Table III. The first column shows the calculated stabilization energy of the lone pair as bending occurs. It should be noted here that the HAH angle in the pyramidal molecules was taken as 109.5° for the sake of uniformity and lack of good data for several of the molecules. In column 2 are the inversion barriers for the molecules obtained from the various methods shown. The agreement between the trends of the stabilization energy and those of the inversion barrier are remarkable.

An alternative approach would be to partition the AH_3 molecule into two fragments: the A atom and H_3 taken in the appropriate geometry. One can then recombine these fragments and, using second-order perturbation theory,[5] calculate the stabilization energy for the planar and pyramidal forms of the molecule. The energy ordering of the interacting MO's, i.e., the AO's of A and the group MO's of H_3 (HGMO's), can only be qualitatively assessed from knowledge of valence-state ionization energies of A and H. The interaction diagrams[12] for planar NH_3 and PH_3 shown in Figure 3 have been constructed with reference to known ionization potentials of the neutral atoms[13] and assuming the splitting of the hydrogen GMO's is small compared with the difference between the ionization potentials of the atoms.

In the planar geometry, the lowest HGMO (ϕ_1) can only mix with the valence s AO on A thus forming the $1A_1$ and $2A_1$ MO's of the molecule. Similarly, the degenerate pair of

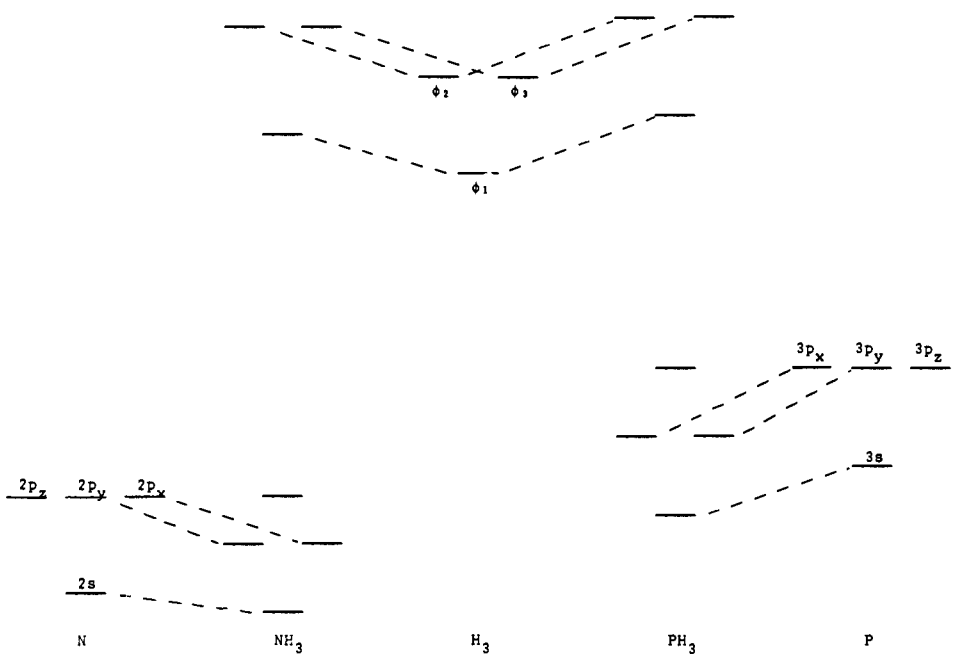

Figure 3. The interaction diagrams for NH_3 and PH_3 in their planar geometry. The fragments used to construct the molecules are the central-atom AO's and the hydrogen-group MO's.

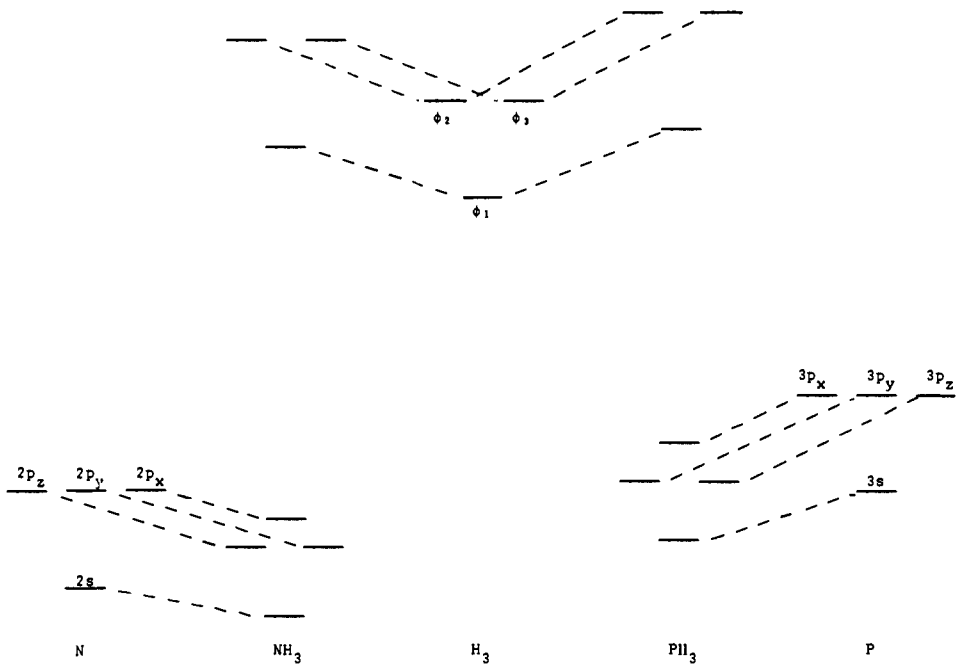

Figure 4. The interaction diagram for NH_3 and PH_3 in their pyramidal geometry. The fragments used to construct the molecules are the central-atom AO's and the hydrogen-group MO's.

HGMO's each interact with the p_x AO and p_y AO of A to form the 1E′ and 2E′ MO's of the molecule. As expected, the p_z AO of A does not mix with a HGMO and represents the lone pair AO. The qualitative ordering of the resulting MO's of the complete AH_3 molecule agrees with those obtained in our explicit CNDO/2 calculations and with calculations of others.[11,14]

The analogous interaction diagram for the pyramidal molecules is shown in Figure 4.[12] The interactions are qualitatively the same, except now the p_z AO can interact with the lowest HGMO (ϕ_1). However, before considering this interaction in detail, we will consider the changes in the other interactions common to both geometries.

The mixing between ϕ_1 and the valence s AO of A remains almost unchanged in the planar and pyramidal forms of the molecule. However, the interaction of ϕ_2 and ϕ_3 with the valence p AO's of A will be decreased in the pyramidal molecule due to the decrease in overlap. The decrease in the p_x-ϕ_2 and p_y-ϕ_3 interactions can be evaluated using eq 3. We shall consider only the p_x-ϕ_2 interaction, but the results will be the same for the p_y-ϕ_3 interaction. Using eq 3, the change in the interaction is given by

$$SE_{pl} - SE_{py} = \frac{k^2}{\Delta E}(S_{pl}^2 - S_{py}^2) \qquad (5)$$

where SE_{pl} and SE_{py} are the lowering in energy of the p_x

AO due to its interaction with ϕ_2 in the planar and pyramidal geometries, respectively. We have evaluated the necessary overlap integrals for both forms of NH_3 and PH_3 by using the atomic overlap integrals from our CNDO/2 calculations. These are given below along with the $S_{pl}^2-S_{py}^2$ term.

	NH_3	PH_3
S_{pl}	0.5346	0.6207
S_{py}	0.2493	0.5083
$S_{pl}^2 - S_{py}^2$	0.2236	0.1269

From these results, we can conclude that the planar forms of both PH_3 and NH_3 will be favored by this interaction. Now, the overlap term will tend to favor a greater preference for the planar form in NH_3 while the energy separation term will tend to favor a greater preference for the planar form in PH_3. Actually, the overlap factor changes faster than the energy-separation factor and this interaction would favor greater pyramidal preference for PH_3. However, the effect is likely to be small.

Returning now to the $Ap_z-\phi_1$ interaction, we see from Figure 4 that this interaction will be greater in the PH_3 case than in the NH_3 case. This is due to a smaller energy separation and greater overlap of Pp_z and ϕ_1 as compared with Np_z and ϕ_1. It should be mentioned that the HGMO's in both molecules will not be exactly the same. In particular, the splitting is expected to be larger in the N case than in the P case. However, this slight difference will be small compared with the difference between the ionization potentials of the N p_z AO and P p_z AO.

In short, the key interaction which is responsible for the greater pyramidal preference of PH_3 vs. NH_3 is the $p_z-\phi_1$ interaction, a conclusion also reached on the basis of the previous alternative approach.

Any change in the system that will increase the interaction between the HOMO and the LUMO in these AH_3 molecules will increase the barrier to inversion. Such a change can be effected by altering the electronegativity of the substituents. The change in energy of an MO upon introduction of a more electronegative substituent and due solely to the inductive effect of this substituent is given by the expression[5]

$$\Delta\epsilon_\mu = \sum_i a_{\mu i}^2 \Delta\alpha_i \tag{6}$$

where $\Delta\epsilon_\mu$ is the change in energy of the μth MO, $\Delta\alpha_i$ is the change in the Coulomb integral, and $a_{\mu i}$ is the coefficient of the ith AO in the μth MO. As the electronegativity of the substituent is increased, the LUMO should decrease in energy. This decrease allows a greater interaction between the HOMO (which will not decrease in energy since it is a pure p AO on the central atom) and the LUMO. The increase in the inversion barrier in NH_3 as the electronegativity of hydrogen is artificially increased has been demonstrated by the ab initio calculations of Mislow, Rauk, and Allen.[15] Experimental results supporting these theoretical conclusions are shown by entries c to f in Table I, where the change from a methyl or methylene group to a hydroxy or oxygen, respectively, doubles the barrier. Undoubtedly, part of this increase in the barrier of NR_2OH relative to that of NR_2CH_3 is due to π-type conjugative effects. This point is illustrated by the interaction diagram of Figure 5. In the case of CH_3-NR_2, the four-electron destabilizing $\phi_1-\chi_0$ interaction as well as the two-electron $\phi_2-\chi_0$ interaction increase as one goes from pyramidal to planar form and tend to counteract each other. These effects can be easily understood by reference to the expressions (including overlap) for the two-electron stabilization,[16] $\Delta\epsilon^2$, and four-electron de-

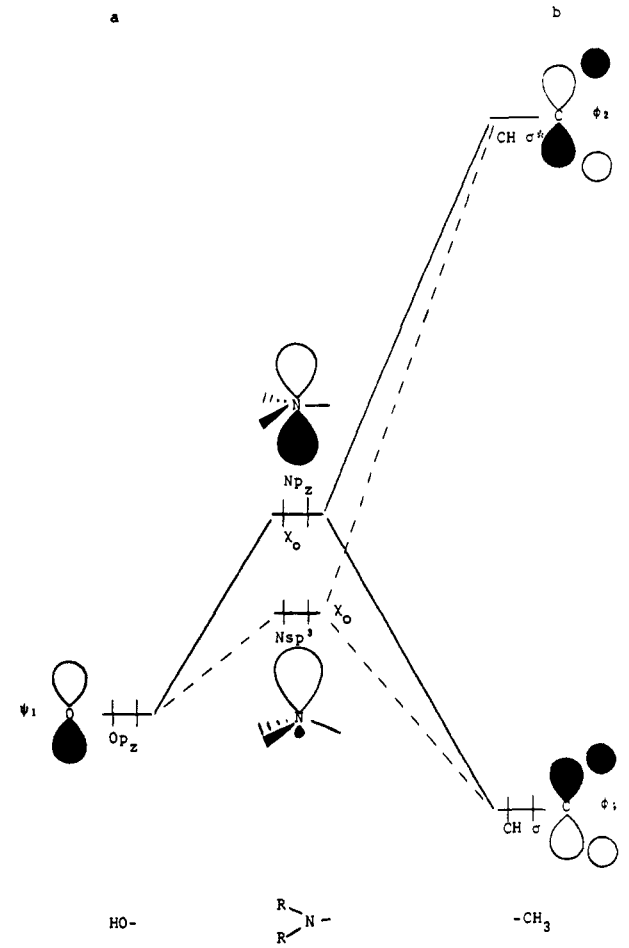

Figure 5. Dominant orbital interactions in planar (solid lines) and pyramidal (broken lines) substituted amines: (a) R_2N-OH; (b) R_2N-CH_3.

stabilization,[17] $\Delta\epsilon^4$, given below.

$$\Delta\epsilon^2 = \frac{(k-E_2)^2 S_{02}^2}{E_0 - E_2} \tag{7}$$

$$\Delta\epsilon^4 = \left[\frac{E_0+E_1}{2} - k\right]\left[\frac{4S_{01}^2}{1-S_{01}^2}\right] \tag{8}$$

As the nitrogen center is transformed from pyramidal to planar the following changes occur: (a) E_0 increases and, thus both $E_0 - E_2$ and $(E_0 + E_1)/2$ decrease, while $k - E_0$ increases; (b) both S_{01} and S_{02} increase. These changes give rise to an increased $\Delta\epsilon^2$ as well as an increased $\Delta\epsilon^4$, the two effects tending to cancel each other. On the other hand, there is only a four-electron destabilizing $\psi_1-\chi_0$ interaction in the case of NR_2OH which increases as the molecule becomes planar, for reasons which are the same as the ones discussed in the previous case. Hence, π-type conjugative effects also predict a higher barrier in NR_2OH relative to NR_2-CH_3. However, the electronegativity effect is certainly responsible for some part of the increase. Numerous other examples of this "electronegativity effect" have been noted, although the accompanying π conjugative effect is also present.[18]

Finally, we wish to emphasize a particularly valuable use of the ideas presented in this paper relating to the construction of Walsh diagrams.[4] If the eigenvalues of the valence MO's for the planar AH_3 molecule are known, one can construct the Walsh diagram just by considering overlap arguments. Recognition of the importance of the energy-separation term in determining the magnitude of the MO interactions, as illustrated in this paper, can lead to a qualitative

prediction of the changes of the Walsh diagram due to a change of the central atom A.

These qualitative ideas can be used to understand the inversion barrier in AH_3 radicals and their substituted analogues as well as barriers to pyramidalization in AH_3 cations and their substituted analogues.[19]

Acknowledgment. We wish to thank the donors of the Petroleum Research Fund administered by the American Chemical Society, and the Research Corporation for partial support of this research.

References and Notes

(1) J. Lambert, *Top. Stereochem.*, **6**, 19 (1971).
(2) J. D. Swaken and J. A. Ibers, *J. Chem. Phys.*, **36**, 1914 (1962).
(3) J. M. Lehn and B. Munsch, *Chem. Commun.*, 1327 (1969).
(4) A. D. Walsh, *J. Chem. Soc.*, 2260 (1953), and paper thereafter; B. M. Gimarc, *J. Am. Chem. Soc.*, **93**, 593 (1971).
(5) M. J. S. Dewar, "The Molecular Orbital Theory of Organic Chemistry", McGraw-Hill, New York, N.Y., 1969.
(6) H. C. Longuet-Higgins and M. de V. Roberts, *Proc. R. Soc. London, Ser. A*, **224**, 336 (1954); **230**, 110 (1955); R. Hoffmann and W. N. Lipscomb, *J. Chem. Phys.*, **36**, 2179, 3489 (1962); **37**, 2872 (1962); R. Hoffmann, *ibid.*, **40**, 2745 (1964).
(7) Similar reasoning is apparent in a treatment of AX_2 molecules in W. T. Borden, "Modern Molecular Orbital Theory for Organic Chemists", Prentice-Hall, Englewood Cliffs, N.J., 1975, p 136, footnote 1.
(8) J. A. Pople and D. L. Beveridge, "Approximate Molecular Orbital Theory", McGraw-Hill, New York, N.Y., 1970. The d orbitals were suppressed in the calculations of the third-row elements.
(9) L. S. Bartell and R. C. Hirst, *J. Chem. Phys.*, **31**, 449 (1959); E. D. Palik and E. E. Bell, *ibid.*, **26**, 1093 (1951).
(10) J. M. Lehn, A. Veillard, and B. Munsch, *Theor. Chim. Acta*, **9**, 275 (1968).
(11) J. M. Lehn and B. Munsch, *Mol. Phys.*, **23**, 91 (1971).
(12) The interaction between the Ap_z AO and ϕ_1 and the interaction between the As AO and ϕ_1 gives rise to a coupling. This coupling is manifested by a small repulsion between the $(Ap_z + \phi_1)$ MO and the $(As + \phi_1)$ MO initially formed by the union of the A atom and H_3 fragment. For this reason, the lone pair orbital in the pyramidal molecule is higher in energy than the degenerate pair of MO's. Since overlap has been neglected, this repulsion has no net energetic effect. In general, neglect of overlap is justified because two electron-stabilizing effects are more important than four electron-destabilizing effects.
(13) J. Hinze and H. H. Jaffe, *J. Am. Chem. Soc.*, **84**, 540 (1962).
(14) L. C. Allen, E. Clementi, and A. Rauk, *J. Chem. Phys.*, **52**, 4133 (1970).
(15) L. C. Allen, A. Rauk, and K. Mislow, *Angew. Chem.*, **9**, 400 (1970).
(16) The expression for the two-electron stabilization is obtained from perturbation theory with inclusion of overlap; for example, see: L. Salem, *J. Am. Chem. Soc.*, **90**, 543 (1968). The qualitative trend remains the same whether overlap is included or neglected (e.g., see eq 2).
(17) The expression for the four-electron destabilization is obtained by solving the two orbital-four electron interaction problem variationally; for example, see: N. C. Baird and R. M. West, *J. Am. Chem. Soc.*, **93**, 4427 (1971); K. Müller, *Helv. Chim. Acta*, **53**, 1112 (1970). Here inclusion of overlap is necessary to get the correct trend since, when overlap is neglected, ΔE^4 is always zero.
(18) J. M. Lehn, *Fortschr. Chem. Forsch.*, **15**, 311 (1970).
(19) N. D. Epiotis and W. R. Cherry, to be submitted for publication.

Molecular Dynamics of the Hydrogen Iodide and Hydrogen–Iodine Exchange Reactions

R. L. Jaffe, J. M. Henry, and J. B. Anderson*

Contribution from Yale University, New Haven, Connecticut 06520.
Received March 12, 1975

Abstract: A combined phase-space/trajectory study of the hydrogen iodide ($HI + HI \rightarrow H_2 + I_2$) and the hydrogen–iodine ($H_2 + I_2 \rightarrow HI + HI$) exchange reactions was carried out using the semiempirical potential energy surface derived by Raff et al. From a minimum of computation effort the calculations yield overall reaction rates and mechanisms, reactant and product configurations, and energy distributions among reactants and products for thermal reactants at 700 K. The exchange reactions are found to occur through both the C_{2v} trapezoidal and the symmetric linear transition configurations of the potential energy surface used. In reaction of HI + HI via the trapezoidal configuration only stable H_2 and I_2 occur as products. In reaction via the linear configuration the products are primarily stable H_2 molecules and separated I atom pairs with lesser amounts of stable and quasibound I_2 molecules. The calculated overall rate is approximately $\frac{1}{10}$ that from experimental measurements. With adjustment of the relative barrier heights for the two transition configurations to favor the atomic mechanism ($H_2 + 2I \rightarrow HI + HI$) it may be possible to produce agreement with Sullivan's photochemical experiments. The calculated vibrational excitation of reacting HI molecules is in accord with experimental measurements by Jaffe and Anderson. Where directly comparable the results are in agreement with those of a standard quasiclassical trajectory study by Raff et al. However, in the work by Raff et al. a complete statistical investigation of the reactions $H_2 + I_2 \rightarrow HI + HI$ and $H_2 + 2I \rightarrow HI + HI$ was precluded by excessive computer time requirements and the rates of these reactions were underestimated.

Preface

This paper gives a full account of the application of the combined phase-space/trajectory method to the hydrogen iodide and hydrogen–iodine exchange reactions. A summary[1] of results of this study has been published previously. More recent calculations[2] by identical procedures with a modified potential energy surface have also been reported. In these it was found that adjustment of the potential energy surface to promote reaction of HI with HI via a collinear configuration led to reaction products molecular hydrogen [H_2] and either separated iodine atoms [I + I] or molecular iodine vibrationally excited near the dissociation limit [I_2 (hi v)]. It was concluded that slight additional modification of the potential energy surface might favor either set of reaction products.

The validity of the combined phase-space/trajectory method has now been demonstrated for a number of systems[3-7] and is regarded by some as obvious.[8] The calculations reported in the main body of this paper are supplemented by a larger number of conventional trajectories for $H_2 + I_2$ encounters likely to produce reaction as indicated by the combined phase-space/trajectory results. Although there is a large statistical uncertainty in any of the properties calculated for the supplemental set of trajectories, there is essential agreement with the results of the combined phase-space/trajectory method.

*Address correspondence to Department of Chemistry, The Pennsylvania State University, University Park, Pa. 16802.